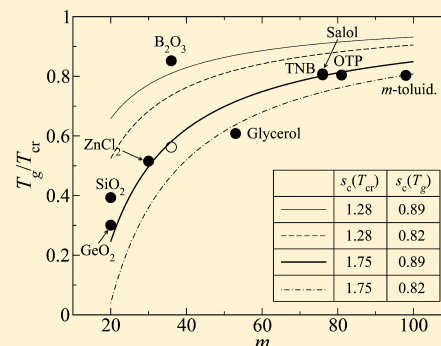


Liquid State Elasticity and the Onset of Activated Transport in Glass Formers

Pyotr Rabochiy[†] and Vassiliy Lubchenko^{*,†,‡}Departments of [†]Chemistry and [‡]Physics, University of Houston, Houston, Texas 77204-5003, United States

ABSTRACT: We show that the crossover temperature to activated transport in glass-forming liquids can be predicted using their finite-frequency elastic constants and the fusion entropy. The latter quantities determine the size of the vibrational motions of chemically rigid molecular units in the liquid as a function of temperature. Using the notion that, at the crossover, the “Lindemann ratio” of this vibrational displacement to the corresponding lattice spacing is nearly system-independent, one can estimate the crossover temperature. For nine specific substances, the resulting predictions are consistent with experimental estimates of the dynamical crossover temperature and also with the predictions of the random first order transition (RFOT) theory for the onset of barrierless transport owing to fractal correlated rearrangements that occur at a critical configurational entropy. In particular, the fragility index is found to inversely correlate with the ratio of the crossover and glass transition temperatures. This prediction agrees with most observations except for boron oxide B_2O_3 , which deviates from the common trend. This exception is argued to result from additional local ordering with lowering temperature in B_2O_3 . Finally, we show that taking into account the temperature dependence of the elastic constants is crucial for accurate estimates of the crossover temperature.



I. INTRODUCTION

The structural glass transition takes place when a liquid fails to equilibrate during cooling and/or compression; as such, it is not a thermodynamic phase transition. Instead, the structural glass transition is defined kinetically, usually by specifying the relaxation rate which was exceeded when the liquid was quenched. To understand the structural glass transition one must explain how the relaxation barriers *above* the glass transition form and what the ensuing particle motions are. Most conventional glass-forming liquids can be realistically quenched only when the transport is already activated. In contrast, for colloidal suspensions the motions of the suspended particles are already slowed by friction with the solvent so much that the transport remains collisional even on the longest observation times achievable in the laboratory.

Liquid transport near the glass transition, for conventional laboratory glass formers, is realized by rare, activated events when the typical relaxation time generically exceeds the vibrational relaxation time by three or more orders of magnitude, that is, at viscosities above 10 Ps or so.^{1–4} This time scale separation ensures that a given particle faces the same neighbors for multiple vibrational relaxation times, implying that the translational symmetry is broken on the time scale of molecular vibrations. In other words, the usual assumption about the uniformity of the liquid density profile does not hold. In the contrasting picture of collisional transport, which is valid at higher temperatures, the density profile may be thought of as uniform: An individual particle is subject to a configurationally averaged-out force stemming from collisions with many particles that are not necessarily part of its immediate coordination shell. It is the (transient) translational

symmetry breaking—which results in the emergence of the activated transport—that is the fundamental change underlying the glass transition, not the kinetic arrest at T_g . The change is not mathematically sharp because the symmetry breaking occurs locally,⁵ and so one must speak of a *crossover* between the collisional and activated transport rather than a singularity. Although these basic notions appear to be generally recognized, there is less agreement about the precise mechanism of the crossover. Likewise there are disputes about the exact temperature to be ascribed to the crossover.^{6,7}

Identifying the temperature range for the crossover to the activated transport regime is important for several relatively distinct reasons, including: (1) The interval's center, call it T_{cr} , is an equilibrium material property, just as are the melting and boiling temperatures. As such, the crossover temperature T_{cr} is necessary for a full description of the physical chemistry of a substance. (2) To generate a realistic picture of a laboratory glass in a computer simulation, the melt must at least be equilibrated to a temperature $T < T_{cr}$ before quenching. Important properties of laboratory glasses are known to be exquisitely sensitive to the atomic positions, such as the midgap electronic states responsible for electronic and optical anomalies in amorphous chalcogenides.^{8–10} (3) Both in the experiment and computer simulation, it is necessary to reach below T_{cr} to properly identify the cooperative events and their extent and other parameters that can be used to test alternative theories of such glassy phenomena. In their simplest form,

Received: January 19, 2012

Revised: March 19, 2012

Published: April 25, 2012

distinctly different theories apply either above or below T_{cr} ; thus, one must know this temperature to make meaningful comparisons of particular simplified theories with observation.

The crossover to activated transport was first identified by Stoessel and Wolynes¹¹ in 1984 and a bit later in a more formal treatment by Singh, Stoessel, and Wolynes¹² (SSW); see also related studies in refs 13 and 14. SSW use an ansatz for the particle density distribution function for a collection of hard spheres:

$$\rho(\mathbf{r}, \alpha) = (\alpha/\pi)^{3/2} \sum_p e^{-\alpha(\mathbf{r}-\mathbf{R}_p)^2} \quad (1)$$

to estimate the free energy $F(\alpha)$ of the liquid as a function of an effective force constant α . The points \mathbf{R}_p were taken to be arranged in an aperiodic lattice like the mechanically stable aperiodic lattice constructed decades earlier by Bernal.¹⁵ In the meanfield limit, the onset of the activated transport is signaled by the emergence of a metastable minimum in $F(\alpha)$ at $\alpha > 0$, which occurs above a certain density. When the particles are not infinitely rigid, the emergence of metastable minima can be also induced by lowering the temperature and/or compression.¹⁶ The corresponding temperature is often called T_A . In actual liquids, fluctuations in the order parameter α shift the onset of the activated transport¹ to higher densities, at which the metastable minimum is sufficiently deep to contain the fluctuations; at the same time, the transition becomes a gradual crossover, as already mentioned.

The longevity of aperiodic structures exhibits itself most directly in liquid response functions—such as the intermediate scattering function in neutron echo spectroscopy¹⁷—via a plateau following the vibrational relaxation portion. In a glass or deeply supercooled liquid, the plateau's length greatly exceeds the vibrational relaxation time. The dynamic crossover temperature T_c of the mode-coupling theory^{18,19} (MCT) has been inferred from such measured response functions, usually in the frequency domain; see the review in ref 4. The temperature T_c corresponds to the temperature T_A in the meanfield limit²⁰ and is thus clearly related to the crossover temperature; however, the precise relation between T_c and T_{cr} is less obvious. The determination of T_c from experimental data depends on the detailed MCT-inspired functional form of the relaxation profile used for curve-fitting.

The plateau is also observed in simulations; its interpretation is subject to finite size effects and potential lack of equilibration at the large time-scale separation needed for the metastable structures to be well-defined. Similarly difficult is monitoring the emergence of activated transport via *spatial* cooperativity that should, presumably, accompany the crossover. It is not straightforward to identify a local order parameter for a Hamiltonian not defined on a static lattice,²¹ since the crossover is not accompanied by a point group symmetry or volume change. Existing approaches have monitored overlaps between different configurations based on populations of small cells that fill the sample.²² Again, monitoring spatial correlations between density fluctuations may be complicated by detailed boundary conditions and other finite-size effects.^{23,24} In addition, there is also the possibility of phase separation or chemical ordering as supercooled liquids are usually modeled with mixtures whose ground state is in all likelihood a mixture of periodic-crystalline phases. Finally, simulations of actual liquids requires good knowledge of the interactions. We must acknowledge that fully realistic

interactions are often more complex and even more computationally expensive to study than are the common model liquids, such as Lennard–Jones mixtures.

A purely theoretical analysis of stability of the compact activated transitions between distinct metastable structures in comparison with fractal or string-like collisional events, by Stevenson et al.,³ suggests that the configurational entropy should have a universal value at the crossover. This prediction was employed by those authors to estimate the crossover temperature using the measured glass transition temperature T_g or the estimated Kautzmann temperature along with the heat capacity jump at T_g .

Here we develop a method of predicting the crossover temperature for actual substances that does not rely on direct simulations. The crossover temperature, which is related within microscopic theory to the detailed interparticle interactions, can be estimated using only measured elastic constants (at high but finite frequency) and fusion entropy. We utilize the notion that, at the crossover, a particle samples with equal likelihood the uniform liquid and the metastable aperiodic states; the uniform liquid and the degenerate aperiodic crystal are thus at equilibrium, even though there is no phase separation. As anticipated already a century ago by Lindemann²⁵ and in more recent studies of systems with relatively simple interactions,^{12,26,27} the particle vibrational displacement should be a nearly universal quotient of the lattice spacing at solid–liquid equilibrium.²⁸ This notion has been confirmed by recent analysis of the pressure dependence of the crossover for Lennard–Jones (LJ) liquids with tunable coordination.¹⁶

A connection between the latter Lennard–Jones system and actual substances—which have more complicated interactions—can be made by estimating the magnitude of local vibrational motions at the wavelength that corresponds to the size of a chemically rigid molecular unit, which is not disturbed by the reconfigurational motions of the liquid. The crossover can then be found by equating this vibrational displacement to its known value in the simple LJ system. In contrast with most ways to determine T_c which use kinetic measurements, the present method of determining the onset of activated transport is based exclusively on *thermodynamical* considerations; at the same time, some parallels with the work of Stevenson et al.³ can be drawn.

The article is organized as follows: In Section 2 we present a simple approximation that allows one to estimate the typical vibrational displacement at wavelengths exceeding the size of the chemically rigid unit; the input quantities are the measured speed of sound and fusion entropy. A simple formula for T_{cr} is derived based on the near universality of the Lindemann ratio. In Section 3, we compare the predicted T_{cr} for several actual substances with experimental estimates of this quantity and also predictions of the random first-order transition (RFOT) theory based on fractal or string excitations.²⁹ We find reasonable agreement of this elasticity based theory with the other estimates for all substances except for boron oxide B_2O_3 ; this deviation is argued to stem from a gradual change in local ordering with temperature. The final Section 4 summarizes the present findings.

II. CORRESPONDENCE BETWEEN ACTUAL LIQUID AND REFERENCE LIQUID WITH WEAK INTERACTIONS

First, we calculate the one-particle density distribution function on time scales such that the particles can be regarded as part of

a stable 3D lattice. Consider a distribution function $\sum_p \delta(\mathbf{r} - \mathbf{r}_p)$, where \mathbf{r}_p correspond to the *instantaneous* particle locations. Likewise, we can consider an arrangement where the points $\{\mathbf{r}_p\}$ correspond to the locations of chemically rigid units, or “beads,” which are not necessarily tied to actual particles, but rather centers of mass of (small) groups of atoms. Our aim is to obtain the thermal average of the expression $\sum_p \delta(\mathbf{r} - \mathbf{r}_p)$ with respect to deviation \mathbf{u}_p of the instantaneous values of the coordinates \mathbf{r}_p from their average values \mathbf{R}_p : $\mathbf{r}_p = \mathbf{R}_p + \mathbf{u}_p$. The points $\{\mathbf{R}_p\}$ are assumed to form a uniform aperiodic lattice with a number density ρ .

We treat our solid, in the simplest fashion, as a harmonic continuum subject to the energy functional:^{30,31}

$$H = \frac{1}{2} \Lambda_{ijlm} \int u_{ij} u_{lm} d^3\mathbf{R} \quad (2)$$

where the standard deformation tensor u_{ij} is defined as

$$u_{ij} \equiv (1/2)(\partial u_i / \partial x_j + \partial u_j / \partial x_i) \quad (3)$$

Everywhere below we assume isotropic elasticity,³⁰ which should be adequate for amorphous lattices on length scales above the bead size, as the latter must exceed²¹ the atomic size:

$$\Lambda_{ijlm} = K \delta_{ij} \delta_{lm} + \mu [\delta_{il} \delta_{jm} + \delta_{im} \delta_{jl} - (2/3) \delta_{ij} \delta_{lm}] \quad (4)$$

Here K and μ are the bulk and shear modulus, respectively. Note that since K and μ describe individual metastable minima of the liquid, they refer to *finite* frequency moduli, which can be conveniently measured via sound speeds. (Clearly, the zero frequency shear modulus in a liquid is zero, while $K(\omega = 0)$ is generally distinct from its finite-frequency counterpart.)

The discreteness of the lattice can be approximately accounted for by implementing a sharp ultraviolet cutoff at the wave vector $\pi \rho^{1/3}$, as in the Debye phonon theory. By construction, we are agnostic as to the motions on length scales smaller the volumetric size a of the bead. By the RFOT theory,^{5,12,29,32,33} the activated dynamics in liquids can be thought of as local interconversion between the distinct metastable aperiodic structures. Bevzenko and Lubchenko²¹ have put forth an explicit field theory that governs such interconversions, where the ultraviolet cutoff is, again, determined by a bead size.

The aim is thus to compute the thermally averaged instantaneous distribution function $\sum_p \delta(\mathbf{r} - \mathbf{r}_p) \equiv \sum_p \delta[\mathbf{r} - (\mathbf{R}_p + \mathbf{u}_p)]$, where the deviations \mathbf{u}_p from the mean particle positions are subject to Hamiltonian (2):

$$\begin{aligned} \rho(\mathbf{r}) &= \langle \sum_p \delta(\mathbf{r} - \mathbf{r}_p) \rangle_H \\ &= \frac{1}{(2\pi)^3} \sum_p \int e^{-i(\mathbf{r} - \mathbf{R}_p) \cdot \mathbf{b}} \langle e^{i\mathbf{u}_p \cdot \mathbf{b}} \rangle_H d^3\mathbf{b} \end{aligned} \quad (5)$$

Note that if \mathbf{r}_p correspond to the atomic coordinates, the angular-bracketed expression in the equation above is simply the Debye–Waller factor.

A standard calculation, see for example ref 21 and Chapter 138 of ref 34, yields

$$\langle e^{i\mathbf{u}_p \cdot \mathbf{b}} \rangle_H = \exp \left[-b_s b_t \frac{k_B T}{2} \int \frac{d^3\mathbf{k}}{(2\pi)^3} L_{st}^{-1}(\mathbf{k}) \right] \quad (6)$$

where

$$L_{st} = \Lambda_{slmt} k_l k_m \quad (7)$$

and

$$L_{st}^{-1} = \frac{1}{\mu k^2} \left(\delta_{st} - \frac{3K + \mu}{3K + 4\mu} \frac{k_s k_t}{k^2} \right) \quad (8)$$

That $L_{st} L_{jt}^{-1} = \delta_{st}$ can be checked directly. Using π/a as the ultraviolet cutoff in the k -integral in eq 6 readily yields:

$$\langle e^{i\mathbf{u}_p \cdot \mathbf{b}} \rangle_H = e^{-b^2/4\alpha} \quad (9)$$

where

$$\alpha^{-1} \equiv \frac{1}{a} \frac{k_B T}{3\pi\mu} \frac{6K + 11\mu}{3K + 4\mu} \quad (10)$$

Substituting expression 9 into eq 5 and integrating over \mathbf{b} yields expression 1, that is, the one particle distribution function in a solid is given precisely by a superposition of Gaussians, in the harmonic approximation.

Furthermore, in view of $\rho \equiv 1/a^3$, the equation above yields

$$\alpha \rho^{-2/3} = \frac{3\pi\mu}{\rho k_B T} \frac{3K + 4\mu}{6K + 11\mu} \quad (11)$$

that is, the effective spring constant α is determined by the elastic moduli, density, and temperature T . Note the dimensionless quantity on the lhs is equal, up to a factor of order one, to the inverse square of the ratio of the typical vibrational displacement of a particle to the lattice spacing.³⁵ Although the result of a detailed calculation, eq 11 is essentially a restatement of the equipartition theorem: According to eq 2, $\Lambda_{ijlm} \langle u_{ij} u_{lm} \rangle / \rho$ gives the average potential energy per bead. For a harmonic lattice, this should be equal to $k_B T$, up to a factor of order one; see also ref 36.

We have thus established that in the appropriate range of wavelengths, the lattice can be thought of as composed of particles obeying the isotropic Gaussian density distribution from eq 1. This finding suggests that a straightforward connection can be made with density functional theory (DFT) treatments of liquid-to-solid transitions of simpler, model liquids. Indeed, these treatments routinely take the isotropic Gaussian density distribution as the density ansatz, with the aim of estimating the free energy $F(\alpha)$ as a function of the effective spring constant α . The emergence of a solid is signaled by the appearance of a minimum in $F(\alpha)$. Furthermore, our recent study¹⁶ of the onset of activated transport in Lennard–Jones liquids with tunable coordination indicates that the crossover occurs at a nearly universal value of the Lindemann parameter defined here as in ref 26:

$$L \equiv \langle r^2 \rangle^{1/2} / r_{nn} = (3/2\alpha)^{1/2} / r_{nn} \quad (12)$$

The quantity r_{nn} stands for the spacing between the nearest neighbors, which is not uniquely defined for an aperiodic lattice. In our earlier paper,¹⁶ we put forth a specific prescription for determining the spacing based on the direct correlation function. This prescription yields

$$r_{nn} \approx 1.14/\rho^{1/3} \quad (13)$$

This length is about one percent larger than the nearest neighbor distance in the face-centered cubic lattice at the same density ρ . In that work, we also argued that the value of the Lindemann ratio at the crossover temperature should be numerically close to the value of the Lindemann ratio at the triple point of the Lennard–Jones system, that is, approx-

Table 1. Values of the Fragility Coefficient m , Glass Transition Temperature T_g , Melting Temperature T_m , and Fusion Enthalpy ΔH ;^a Bead Number N_b and the Crossover Temperature T_{cr} ;^b Dynamic Crossover Temperature^c; and Coefficients for the Linear Fits of Eq 16^d

	m	T_g (K)	T_m (K)	ΔH (kJ)	N_b	T_{cr} (K)	T_c (K)	c_1	c_2
SiO ₂	20	1500	1995	9.6	0.34	3818	3330, ³⁸ 3700 ¹	140.7	−53.0
GeO ₂	20	810	1389	16.7	0.86	2693	2390–2590 ³⁹	39.0	−10.0
ZnCl ₂	30	378	598	10.24	1.23	733	563 ⁴⁰	40.4	−17.9
B ₂ O ₃	36	536	723	24	2.37	629(953)	800, ⁴¹ 800–900 ⁴²		
glycerol	53	190	291	18.3	4.50	312	225, ⁴³ 223–233, ⁴⁴ 262, ⁴⁵ 288, ⁴⁶ 300 ⁴⁷	30.4	−14.9
TNB	76	340	474	33.3	5.03	422	407, ⁴⁸ 410, ⁴⁹ 415 ⁵⁰	63.3	−46.2
salol	76	220	315	19.3	4.39	272	256, ⁵¹ 263, ⁵² 266, ⁵³ 275 ⁵⁴	44.8	−31.5
OTP	81	246	329	17.2	3.74	306	285, ⁵⁵ 290, ⁵⁶ 293 ⁵⁷	69.7	−51.4
<i>m</i> -toluidine	98	187	242	8.8	2.60	233	216, ⁵⁸ 233 ⁵⁹	62.7	−45.7

^aColumns 1–4: Values of the fragility coefficient m , glass transition temperature T_g and fusion enthalpy ΔH are from ref 60, except for SiO₂, from refs 61 and 62. The melting temperature T_m data are from ref 62, except for TNB and salol from ref 37. ^bColumns 5–6 are computed according to eqs 15 and 16, respectively. For B₂O₃, we provide the T_{cr} value corresponding to the bead count N_b and, in brackets, that corrected for the boroxol rings. ^cColumn 7 contains earlier estimates of the dynamic crossover temperature, denoted here with T_c . The superscripts indicate the sources of the data. ^dColumns 8–9: The coefficients for the linear fits of the lhs of eq 16 in the form of $c_1 + c_2(T/T_g)$, except for B₂O₃; see text.

imately 0.145. As a result, one obtains, by eqs 11, 12, and 13, that at the crossover:

$$\frac{\mu}{\rho k_B T_{cr}} \frac{3K + 4\mu}{6K + 11\mu} \simeq 5.8 \quad (14)$$

where the values of the elastic constants and the density are at $T = T_{cr}$.

Given the temperature dependencies of the elastic constants and the bead density ρ , eq 14 allows one to determine the crossover temperature for any specific substance. Up to some ambiguity stemming from our use of the Debye approximation, the values of the elastic constants can be determined by measuring the transverse and longitudinal speeds of sound. The size of a chemically rigid unit, on the other hand, can be judged from calibrating the fusion entropy of the liquid to that of a weakly interacting liquid.¹ Judging from a survey of several dozen substances,³⁷ the Lennard–Jones liquid is a suitable reference liquid. Specifically, the fusion entropy of Ar, that is, 1.68 k_B per particle was used in that survey:

$$N_b = \frac{\Delta H_m}{1.68 k_B T_m} \quad (15)$$

where ΔH_m and T_m are the fusion enthalpy and temperature, respectively. System-specific corrections to this overall best estimate are expected, especially for substances exhibiting local ordering and in other, more complicated situations.¹⁰ For those (nonpolymeric) glassformers that do not crystallize, the bead count can be determined using the RFOT based prediction that the configurational entropy at the glass transition on the 10⁵ s scale is universally 0.82 k_B per bead.³² With these comments in mind, we express the lhs of eq 14 through the speeds of transverse (v_T) and longitudinal (v_L) sound and replace the approximate equality by the strict equality for concreteness in future use:

$$\frac{M v_T^2}{N_b k_B T_{cr}} \frac{v_L^2}{2 v_L^2 + v_T^2} = 5.8 \quad (16)$$

The quantity M is the mass of the stoichiometric unit, while N_b is the number of beads per that unit. The expression above has an added convenience, compared to eq 14, in that it does not require a knowledge of the temperature dependence of the density.

III. RESULTS AND DISCUSSION

We consider nine specific glass formers: SiO₂, GeO₂, ZnCl₂, B₂O₃, glycerol, salol, TNB, OTP, and *m*-toluidine. For those substances, both the temperature-dependent elastic constants and calorimetric data are available. We were unable to find others. Despite the limited size of the set, the substances in question do cover a wide range of bonding types and fragility values. The material constants are provided in Table 1. The corresponding sources are given in the caption or in the table itself, except for the sound speeds; the latter can be found in the caption of Figure 1.

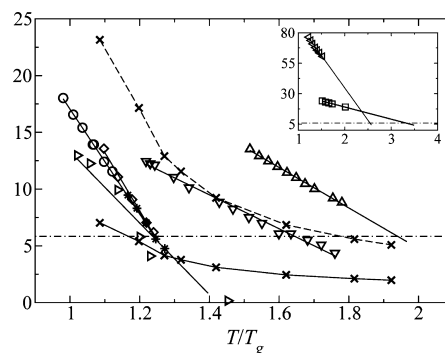


Figure 1. Temperature dependence of the lhs of eq 16. The symbols and references for the T -dependent elastic data are as follows: ZnCl₂ (Δ),⁶³ glycerol (∇),^{64,65} TNB (\circ),⁶⁶ salol (\Diamond),⁶⁷ OTP (\times),^{68,69} *m*-toluidine ($*$),⁷⁰ and B₂O₃ (\times).⁷¹ The sets of data for B₂O₃ correspond to the bead count from eq 15 (solid line) and that corrected for the boroxol rings (dashed line). Inset: same for SiO₂ (\triangleleft)⁷² and GeO₂ (\square).⁷³

The temperature dependence of the lhs of eq 16 for all nine substances is shown in Figure 1. In all cases except B₂O₃, the temperature dependence of the lhs of eq 16 was adequately approximated by a linear function $c_1 + c_2(T/T_g)$; the coefficients c_1 and c_2 are provided in Table 1. Note that in view of the explicit T -dependence in the denominator, this apparent linear behavior implies an appreciable T -dependence of the elastic constants, an important notion we will return to later. Now, the data for B₂O₃ clearly deviate from a straight line; here we simply connected the available data points by straight lines. In two cases, the elastic data were available in a

significantly narrower temperature range than strictly is required for solving eq 16. In those cases, linear extrapolation was employed. Note that this extrapolation may result in significant ambiguity only for the two strongest substances from the set, whose data, incidentally, were plotted separately in the inset because of their larger range compared to the rest of the substances. The resulting values of T_{cr} are listed in Table 1.

First off, we note that the present predictions of the crossover temperature turn out to be consistently above the measured glass transition temperature. This is reassuring, considering that there would appear to be little a priori reason for a complex combination of sound speeds, fusion entropy, and molar mass to consistently produce an energy parameter exceeding T_g . This consistency suggests that the potential sources of ambiguity mentioned above, such as those stemming from our using the Debye vibrational spectrum, do not invalidate the present analysis. The apparent robustness of the present predictions at least for several substances can be traced, formally, to a relatively fast temperature dependence of the lhs of eq 16. In such cases, the resulting prediction of T_{cr} is relatively weakly sensitive to the precise value of the Lindemann ratio or the bead size, for instance. Note that in these cases, the prediction may also be relatively close to the temperature at which the (finite frequency) shear modulus vanishes, as is the case for salol. Nevertheless, for the majority of the substances analyzed here, the temperature dependence of the lhs of eq 16 is not at all slow; such cases serve as a stringent test of the present approach.

To put the present work in the context of earlier work on the onset of cooperative transport in glass-forming liquids we first note that the onset matches most closely the so-called “dynamical crossover.” Novikov and Sokolov⁴ have compiled data on the dynamic crossover temperature in many materials covering a broad range of bonding types and physical properties, including the fragility. Of the nine substances analyzed here, six (those excluding SiO_2 , GeO_2 , and *m*-toluidine) are part of their compilation, while data on *m*-toluidine can be found in refs 58 and 59. Several other approaches to determining a dynamic crossover temperature for these seven substances have been suggested. These give similar but not identical results; we briefly review these methods below.

In one approach, the dynamical crossover temperature is associated with the critical temperature T_c of the mode coupling theory^{18,19} (MCT), at which the plateau in the density–density correlation function⁷⁴ would extend indefinitely (were it not for α -relaxation). By the MCT, the ordinate of the minimum separating the α and β peaks in the imaginary part of the susceptibility function $\chi''(\omega)$ should vanish as $T \rightarrow T_c$. Alternatively, the generalized Debye–Waller factor, which reflects the height of the plateau of the correlation function, behaves nonanalytically below T_c , the nonanalytical portion being proportional $(T_c - T)^{1/2}$. Alternatively, one may determine T_c by fitting measured T -dependencies of the viscosity to the MCT prediction $\tau \propto (T - T_c)^{-\gamma}$.

Relying less on specific theoretically derived fitting forms, the observation of “decoupling” between rotational and translation diffusion has also been associated with a dynamic crossover, which is signaled by an emerging modest difference between the corresponding relaxation times.⁵⁰ Alternatively, Stickel et al.⁷⁵ have proposed to plot the inverse square-root of log-viscosity dependence on $1/T$, which would yield a straight line

for a pure Vogel–Fulcher law but appears to exhibit a kink at a temperature T_b , which is above T_g .

It appears worthwhile to compare the MCT-derived values for T_c with the crossover temperature T_{cr} we determine here: On the one hand, the temperature T_c becomes equivalent to the temperature T_A (at which the metastable structure just begin to form) in the mean-field limit.²⁰ On the other hand, the crossover temperature T_{cr} is the finite-dimensional analogue of T_A (ref 1) and thus is related to T_c , even though the precise relation is not obvious. In addition, some of the MCT-inspired methods of extracting T_c directly refer to the Debye–Waller factor and thereby to the particle vibrational displacement. The present method also directly refers to the vibrational displacement, albeit not necessarily that of individual atoms but, rather, of small groups of atoms. Now, because the temperature for rotational-translational decoupling and the temperature T_b seem to follow closely the temperature T_c , it seems worthwhile to also compare the decoupling temperature T_b with our predicted T_{cr} .

These comparisons are made in Table 1 and are shown, graphically, in Figure 2 with filled symbols. Included in that

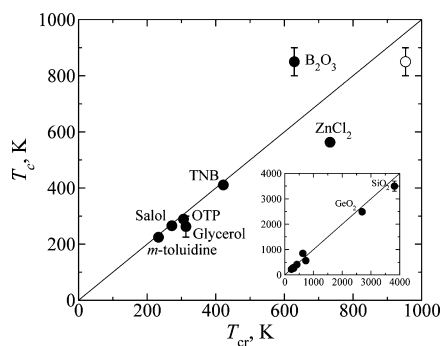


Figure 2. Comparison of the present predictions of the crossover temperature, denoted as T_{cr} and earlier estimates of the dynamic crossover temperature, denoted with T_c . The filled and empty circles for B_2O_3 correspond to the bead count from eq 15 and that corrected for the boraxol rings.

comparison are also silica (SiO_2) and germania (GeO_2), for which experimentally derived crossover temperatures are not available. The depicted range of the previously reported values for SiO_2 is formed by two numbers: one resulting from a simulation by Horbach and Kob,³⁸ the other from fitting the T -dependence of viscosity to the RFOT prediction, by Lubchenko and Wolynes.¹ In the latter case, the crossover temperature has the exact same meaning as in the present study. Finally, the T_c datum for germania is from a simulation-based analysis by Hawlitzky et al.³⁹ Inspection of Figure 2 indicates a strong correlation between earlier and present estimates of the crossover temperature; one conspicuous outlier is boron oxide, to be discussed in due time. To avoid confusion, we reiterate that, despite the discussed connection between T_c and T_{cr} , their precise formal relation or how close their numerical values should be is not entirely clear at present.

Next, we test the numerical values of T_{cr} we have obtained against a simple relation, due to SSW,³ between the crossover temperature (relative to T_K or T_g) and the fragility coefficient

$$m = \left. \frac{\partial \log_{10} \tau}{\partial (T_g/T)} \right|_{T=T_g} \quad (17)$$

Likewise, correlation between T_c and m has also been pointed out earlier.⁷⁶

The RFOT theory predicts for the structural relaxation time τ :^{1,32}

$$\tau = \tau_0 e^{32k_B/s_c} \quad (18)$$

where τ_0 is the vibrational relaxation time, generally a picosecond. Combining this equation with the frequently used functional form for the configurational entropy:⁷⁷

$$s_c(T) = \Delta c_p(T_g) T_g (1/T_K - 1/T) \quad (19)$$

we obtain

$$\frac{T_g}{T_{cr}} = 1 - \frac{1}{m} \left(\frac{s_c(T_{cr})}{s_c(T_g)} - 1 \right) \frac{32k_B}{\ln(10)s_c(T_g)} \quad (20)$$

c.f. the relation between the T_{cr}/T_K ratio and m given in ref 3. Note the correlation above is subject to barrier-softening corrections.¹

To use the RFOT-based formula 20, one needs to specify the configurational entropy at the glass transition and crossover temperatures, per bead. The former depends on the time scale τ of the glass transition, by eq 18. For the sake of argument, here we use two specific values: the often-used value $s_c = 0.82$ ($\tau = 10^5$ s) and $s_c = 0.89$ ($\tau = 1$ h). For the configurational entropy at T_{cr} , we use the value $1.28k_B$ predicted by Stevenson et al.³ and the value $1.75k_B$ suggested by our own analysis of Lennard–Jones systems with tunable coordination.¹⁶ The resulting RFOT-based predictions are shown with continuous lines in Figure 3, while the present estimates are given as filled circles.

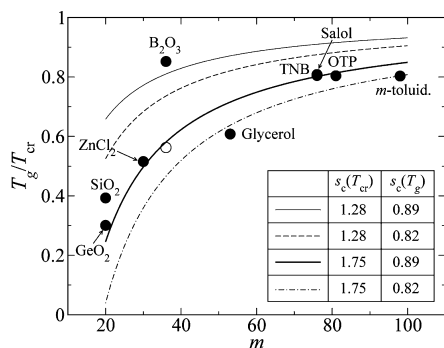


Figure 3. Ratio of the glass transition temperature T_g to the present predictions of T_{cr} plotted against the experimentally determined fragility index m , for the nine substances analyzed here. The filled and empty circles for B_2O_3 correspond to the bead count from eq 15 and that corrected for the boroxol rings. The smooth lines correspond to the prediction of the RFOT theory from eq 20 for specific combinations of the configurational entropy values at T_g and T_{cr} , as listed in the table.

Based on Figures 2 and 3, we conclude that the present predictions of the crossover temperature based on measured elastic properties are in reasonable agreement both with earlier estimates and the predictions of the RFOT theory. One notable outlier is boron oxide B_2O_3 , which we discuss as follows.

In determining the bead count by calibrating the substance's fusion entropy by that of a reference liquid,¹ one assumes that all beads are similar in size and shape. This assumption may not be valid for B_2O_3 . On the one hand, the bead count from Table

1 implies approximately one bead per boron atom, consistent with the chemical intuition that BO_3 units are relatively rigid owing to the strong B–O bond. Consistent with this notion, the B_2O_3 crystal consists of the triangles, each made up of a boron coordinated by three oxygens; see the sketch in Figure 4a. On the other hand, Raman and NMR studies of liquid

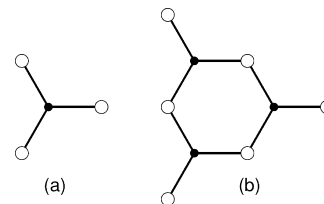


Figure 4. Schematic of the rigid units in liquid B_2O_3 : (a) BO_3 triangles and (b) B_3O_6 boroxol rings. Filled and empty circles represent boron and oxygen atoms, respectively.

boron oxide suggest that, already near the melting temperature, a significant fraction of the liquid is in the form of boroxol rings,⁷⁸ sketched in Figure 4b. This fraction appears to increase upon lowering the temperature and reaches 60%⁷⁸ or even as much as 75%.⁷⁹ The presence of the boroxol rings has been a subject of debate; see a recent review and possible resolution in favor of the significant presence of boroxol in ref 79. Note there is also additional evidence of gradual structural changes in supercooled boron oxide: it exhibits a re-entrant behavior of its elastic moduli with temperature, with a broad minimum above T_g .⁷³

The presence of a significant number of boroxol rings below the melting point implies the chemically rigid unit is on average larger than suggested by the fusion entropy count and that the present estimate of T_{cr} for boron oxide is an underestimate, by eq 16. To assess the degree of underestimation we assume, for concreteness, that the liquid consists exclusively of the BO_3 triangles and B_3O_6 boroxol rings. (As suggested by the fusion entropy, no smaller rigid units are present.) With the assumption that there is one bead per either of these units and the (temperature-dependent) molar fraction of the boroxol is $n(T)$, a heuristic argument in the Appendix suggests the rhs of eq 11 should be corrected upward by a factor $[1 - (2/3)n(T)]^{-2/3}[1 - n(T)(1 - 3^{-1/3})]^{-1}$. The formula $n(T) = 0.88 - 0.30T/T_g$ is a good approximant of the temperature dependence of the boroxol fraction in Figure 9 of ref 78. The crossover temperature estimated using this bead count is given by the empty circles in Figures 2 and 3; it conforms well to the trend exhibited by the other substances.

Finally, we return to the question of how important it is to take into account the temperature dependence of the elastic constants in eq 16. The negative answer would imply that, on one hand, the crossover temperature is largely determined by the properties of the glass itself, in view of the continuous T -dependence of high frequency elastic moduli across the glass transition. On the other hand, it would also imply that we would have available a much larger set of data for tests of the theory. Toward answering this question, we have solved eq 16 under the assumption that the quantities K and μ are temperature-independent and are set to their values at the glass transition. While these solutions, shown in Figure 5, still appear to show some correlation, it is quite poorer than for the T -dependent results. Perhaps more important, the magnitudes of T_{cr} obtained by the two methods differ by as much as a factor

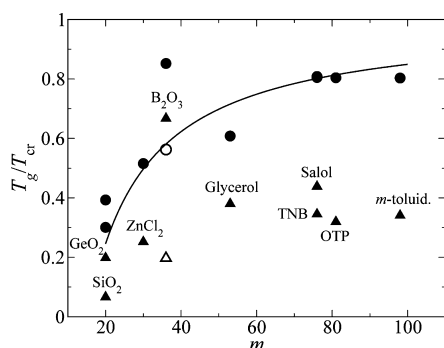


Figure 5. Ratio of the glass transition temperature T_g to the present predictions of T_{cr} plotted against the experimentally determined fragility index m . The circles correspond to the solution of eq 16 and are the same as in Figure 2. The triangles are the solution of that equation under the assumption that the elastic constants K and μ are temperature-independent and set to their values at the glass transition. The smooth line corresponds to $s_c(T_g) = 0.89$ and $s_c(T_{cr}) = 1.75$. As in Figures 1 and 2, the empty symbols correspond to the bead count corrected for the boroxol rings.

of 2. This notion suggests that, for quantitative predictions of T_{cr} , accurate determination of the vibrational displacement is necessary, thus requiring that one take into account the T -dependence of the elastic constants in the liquid.

IV. SUMMARY

We have shown that the temperature of the crossover between collisional and activated transport in actual liquids can be estimated using finite-frequency elastic constants for the liquid and its fusion entropy. At sufficiently high temperatures, the equilibrium profile is uniform, while the transport is largely collisional. At sufficiently low temperatures, the intuitive assumption of the liquid theory on the uniformity of the liquid density profile no longer holds. Each particle is confined to a fixed cage for times greatly exceeding the vibrational relaxation time. Under these conditions, the liquid rearranges by activated transitions between distinct metastable free energy minima. At the crossover between the collisional and activated transport, the particles spend equal time in both regimes.

The crossover temperature is an intrinsic property of a material; its knowledge is just as instrumental in characterizing materials as is the melting temperature, for instance. We note that, for fragile materials, the crossover temperature is below the melting point and, strictly speaking, should be considered as a conditionally equilibrium property. Yet for stronger substances, T_{cr} is consistently above melting and thus can be taken as a true equilibrium property.

The values of the crossover temperature T_{cr} predicted by the present approach turn out to be rather close to the “dynamic crossover temperatures,” which may be associated with the critical temperature T_c of the mode-coupling theory^{18,19} (MCT). The latter temperature is usually found by fitting kinetic data to MCT-predicted functional forms. The agreement is not coincidental since both T_{cr} and T_c are finite-dimensional analogues of the meanfield temperature T_A at which the metastable structures begin to emerge.^{1,20}

Perhaps deeper parallels can be drawn between the present method and the earlier, seemingly different approach by Stevenson, Schmalian, and Wolynes³ (SSW), which is based on the random first-order transition (RFOT) theory.²⁹ These authors have argued the crossover is signaled by the activated

events, which are compact at low temperature, becoming fractal. These fractal rearranging regions correspond to cooperative collisional events that are stringy in shape. (More properly, they resemble percolation clusters.) SSW predict that the crossover occurs at the temperature at which the configurational entropy per rigid chemical unit is equal to a universal number. The necessity to identify the size of the rigid chemical unit, which is often called the “bead,”¹ is another common feature between the present work and ref 3. In the former case, the bead size enters as the ultraviolet cutoff for the continuum-elastic description of an individual metastable state. In the latter, the bead size signifies the appropriate length scale to gauge the entropy content of the liquid.

The bead is relatively straightforward to identify in molecular liquids but less so in covalently bonded materials. Yet identification of the rigid molecular unit is essential for both quantitative description of the supercooled regime and for formulating a field theory for activated transport, in which the bead size plays the role of the ultraviolet cutoff.²¹ In simple terms, the volumetric size of the bead corresponds to the size of the effective Einstein oscillator in a metastable aperiodic solid corresponding to the liquid near the glass transition. It is almost obvious that in simple liquids, such as hard sphere and Lennard–Jones, there is one Einstein oscillator per particle; hereby the coordinates R_p in eq 1 are tied to individual particles. Yet this is generally not the case for more complicated systems such as those exhibiting a high degree of covalent or hydrogen bonding. In the latter case, the vibrations of the effective Einstein oscillator correspond to motions of the center of mass of a *group* of atoms. We have seen that the concrete prescription for finding the bead size through the entropy of fusion yields robust predictions for the crossover temperature, thus supporting in a quantitative way a view of the liquid as a metastable Einstein solid. Conversely, we have seen the presence of additional ordering that could change the identity of the bead with temperature, as seems to be the case with B_2O_3 , calls for refined treatment.

■ APPENDIX A: CORRECTION TO BEAD COUNT IN B_2O_3

The argument leading to eq 10 tacitly assumes the chemically rigid units in the liquid are similar in size and shape, which does not seem to be the case in B_2O_3 . A heuristic way to correct for this bimodal distribution of bead size is to replace the b -integral in eq 6 by a weighted average of two integrals, whereby each weight and the corresponding lower limit of integration refer to the respective bead species. As a result, one gets, in place of eq 10:

$$\alpha^{-1} = \left(n_1 \frac{1}{a_1} + n_2 \frac{1}{a_2} \right) \frac{k_B T}{3\pi\mu} \frac{6K + 11\mu}{3K + 4\mu} \quad (A1)$$

where n_1 and $n_2 = (1 - n_1)$ are the molar fractions of bead species one and two, respectively. At the same time, the effective bead concentration is

$$\rho = n_1/a_1^3 + n_2/a_2^3 \quad (A2)$$

resulting in

$$\alpha \rho^{-2/3} = \frac{[n_1(a_2^3/a_1^3 - 1) + 1]^{-2/3} 3\pi\mu a_2^3}{n_1(a_2/a_1 - 1) + 1} \frac{3K + 4\mu}{k_B T} \frac{3K + 4\mu}{6K + 11\mu} \quad (A3)$$

Supposing species 2 stands for the BO_3 triangle, whose size can be determined calorimetrically, we may take $a_1^3/a_2^3 = 3$, since the boroxol ring contains three times as many borons as the triangle. The first fraction on the rhs of the equation above represents, then, a “correction” to formula 11.

AUTHOR INFORMATION

Notes

The authors declare no competing financial interest.

ACKNOWLEDGMENTS

We thank Peter Wolynes for helpful discussions. We gratefully acknowledge the support by the National Science Foundation (Grant CHE-0956127), the Arnold and Mabel Beckman Foundation Beckman Young Investigator Award, the Alfred P. Sloan Research Fellowship, and the Welch Foundation.

REFERENCES

- Lubchenko, V.; Wolynes, P. G. *J. Chem. Phys.* **2003**, *119*, 9088–9105.
- Casalini, R.; Roland, C. M. *Phys. Rev. Lett.* **2004**, *92*, 245702.
- Stevenson, J. D.; Schmalian, J.; Wolynes, P. G. *Nat. Phys.* **2006**, *2*, 268–274.
- Novikov, V. N.; Sokolov, A. P. *Phys. Rev. E* **2003**, *67* (3), 031507.
- Kirkpatrick, T. R.; Thirumalai, D.; Wolynes, P. G. *Phys. Rev. A* **1989**, *40*, 1045–1054.
- Mallamace, F.; Branca, C.; Corsaro, C.; Leone, N.; Spooren, J.; Chen, S.-H.; Stanley, H. E. *Proc. Natl. Acad. Sci.* **2010**, *107* (S2), 22457–22462.
- Elmatad, Y. S.; Chandler, D.; Garrahan, J. P. *J. Phys. Chem. B* **2010**, *114* (S1), 17113–17119.
- Zhugayevych, A.; Lubchenko, V. *J. Chem. Phys.* **2010**, *132*, 044508.
- Zhugayevych, A.; Lubchenko, V. *J. Chem. Phys.* **2010**, *133*, 234503.
- Zhugayevych, A.; Lubchenko, V. *J. Chem. Phys.* **2010**, *133*, 234504.
- Stoessel, J. P.; Wolynes, P. G. *J. Chem. Phys.* **1984**, *80*, 4502–4512.
- Singh, Y.; Stoessel, J. P.; Wolynes, P. G. *Phys. Rev. Lett.* **1985**, *54*, 1059–1062.
- Baus, M.; Colot, J.-L. *J. Phys. C: Solid State Phys.* **1986**, *19*, L135.
- Lowen, H. *J. Phys.: Condens. Matter* **1990**, *2*, 8477–8484.
- Bernal, J. D. *Proc. R. Soc. Lond. A* **1964**, *280*, 299.
- Rabochiy, P.; Lubchenko, V. *J. Chem. Phys.* **2012**, *136*, 084504.
- Mezei, F.; Russina, M. *J. Phys.: Condens. Mater.* **1999**, *11*, A341.
- Götze, W.; Sjögren, L. *Rep. Prog. Phys.* **1992**, *55*, 241–376.
- Das, S. P. *Rev. Mod. Phys.* **2004**, *76*, 785–851.
- Kirkpatrick, T. R.; Wolynes, P. G. *Phys. Rev. A* **1987**, *35*, 3072–3080.
- Bevzenko, D.; Lubchenko, V. *J. Phys. Chem. B* **2009**, *113*, 16337–16345.
- Cammarota, C.; Cavagna, A.; Giardina, I.; Gradenigo, G.; Grigera, T. S.; Parisi, G.; Verrocchio, P. *Phys. Rev. Lett.* **2010**, *105* (5), 055703.
- Cammarota, C.; Cavagna, A.; Gradenigo, G.; Grigera, T. S.; Verrocchio, P. *J. Stat. Mech.: Theory Exp.* **2009**, 2009 (12), L12002.
- Cavagna, A.; Grigera, T. S.; Verrocchio, P. cond-mat preprint 1006.3746, **2010**, <http://arxiv.org/abs/1006.3746>.
- Lindemann, F. A. *Phys. Z.* **1910**, *11*, 609–612.
- Curtin, W. A.; Ashcroft, N. W. *Phys. Rev. Lett.* **1986**, *56*, 2775–2778.
- Mézard, M.; Parisi, G. *Phys. Rev. Lett.* **1999**, *82* (4), 747–750.
- Lubchenko, V. *J. Phys. Chem. B* **2006**, *110*, 18779–18786.
- Lubchenko, V.; Wolynes, P. G. *Annu. Rev. Phys. Chem.* **2007**, *58*, 235–266.
- Landau, L. D.; Lifshitz, E. M. *Theory of Elasticity*; Pergamon Press: Elmsford, NY, 1986.
- Ashcroft, N. W.; Mermin, N. D. *Solid State Physics*; Harcourt Brace College Publishers: Orlando, FL, 1976.
- Xia, X.; Wolynes, P. G. *Proc. Natl. Acad. Sci.* **2000**, *97*, 2990–2994.
- Lubchenko, V.; Wolynes, P. G. *J. Chem. Phys.* **2004**, *121*, 2852–2865.
- Landau, L. D.; Lifshitz, E. M. *Statistical Mechanics*; Pergamon Press: Elmsford, NY, 1980.
- Denton, A. R.; Ashcroft, N. W. *Phys. Rev. A* **1989**, *39*, 4701–4708.
- Lubchenko, V.; Wolynes, P. G. *Phys. Rev. Lett.* **2001**, *87*, 195901.
- Stevenson, J.; Wolynes, P. G. *J. Phys. Chem. B* **2005**, *109*, 15093–15097.
- Horbach, J.; Kob, W. *Phys. Rev. B* **1999**, *60*, 3169–3181.
- Hawlitzy, M.; Horbach, J.; Ispas, S.; Krack, M.; Binder, K. *J. Phys. Condens. Mater.* **2008**, *20*, 285106.
- Lebon, M. J.; Dreyfus, C.; Li, G.; Aouadi, A.; Cummins, H. Z.; Pick, R. M. *Phys. Rev. E* **1995**, *51*, 4537–4547.
- Engberg, D.; Wischniewski, A.; Buchenau, U.; Börjesson, L.; Dianoux, A. J.; Sokolov, A. P.; Torell, L. M. *Phys. Rev. B* **1998**, *58*, 9087–9097.
- Brodin, A.; Börjesson, L.; Engberg, D.; Torell, L. M.; Sokolov, A. P. *Phys. Rev. B* **1996**, *53*, 11511–11520.
- Wuttke, J.; Hernandez, J.; Li, G.; Coddens, G.; Cummins, H. Z.; Fujara, F.; Petry, W.; Sillescu, H. *Phys. Rev. Lett.* **1994**, *72*, 3052–3055.
- Fransosch, T.; Götze, W.; Mayr, M. R.; Singh, A. P. *Phys. Rev. E* **1997**, *55*, 3183–3190.
- Lunkenheimer, P.; Pimenov, A.; Dressel, M.; Goncharov, Y. G.; Böhmer, R.; Loidl, A. *Phys. Rev. Lett.* **1996**, *77*, 318–321.
- Adichtchev, S.; Blochowicz, T.; Tschirwitz, C.; Novikov, V. N.; Rössler, E. A. *Phys. Rev. E* **2003**, *68*, 011504.
- Rössler, E.; Sokolov, A. P.; Kisliuk, A.; Quitmann, D. *Phys. Rev. B* **1994**, *49*, 14967–14978.
- Bartsch, E.; Debus, O.; Fujara, F.; Kiebel, M.; Petry, W.; Sillescu, H.; Magill, J. *Physica B* **1992**, *180–181*, 808–810.
- Sjögren, L.; Götze, W. In *Dynamics of Disordered Materials*; Richter, D., Dianoux, A. J., Petry, W., Teixeira, J., Eds.; Springer-Verlag: Berlin, 1989; p 33.
- Rössler, E. *Phys. Rev. Lett.* **1990**, *65*, 1595–1598.
- Li, G.; Du, W. M.; Sakai, A.; Cummins, H. Z. *Phys. Rev. A* **1992**, *46*, 3343–3356.
- Toulouse, J.; Coddens, G.; Pattnaik, R. *Physica A* **1993**, *201*, 305–311.
- Yang, Y.; Nelson, K. A. *Phys. Rev. Lett.* **1995**, *74*, 4883–4886.
- Dreyfus, C.; Lebon, M.; Cummins, H.; Toulouse, J.; Bonello, B.; Pick, R. *Physica A* **1993**, *201*, 270–276.
- Gottke, S. D.; Brace, D. D.; Hinze, G.; Fayer, M. D. *J. Phys. Chem. B* **2001**, *105*, 238–245.
- Steffen, W.; Patkowski, A.; Gläser, H.; Meier, G.; Fischer, E. W. *Phys. Rev. E* **1994**, *49*, 2992–3002.
- Petry, W.; Bartsch, E.; Fujara, F.; Kiebel, M.; Sillescu, H.; Farago, B. *Z. Phys. B* **1991**, *83*, 175.
- Mandanici, A.; Cutroni, M.; Richert, R. *J. Chem. Phys.* **2005**, *122*, 084508.
- Aouadi, A.; Dreyfus, C.; Massot, M.; Pick, R. M.; Berger, T.; Steffen, W.; Patkowski, A.; Alba-Simionesco, C. *J. Chem. Phys.* **2000**, *112*, 9860–9873.
- Wang, L.-M.; Angell, C. A.; Richert, R. *J. Chem. Phys.* **2006**, *125* (7), 074505.
- Böhmer, B.; Ngai, K. L.; Angell, C. A.; Plazek, D. *J. Chem. Phys.* **1993**, *99*, 4201–4209.
- CRC *Handbook of Chemistry and Physics*, 91st ed.; Taylor and Francis: London, 2010–2011.
- Dreyfus, C.; Lebon, M. J.; Vivicorsi, F.; Aouadi, A.; Pick, R. M.; Cummins, H. Z. *Phys. Rev. E* **2001**, *63*, 041509.
- Kovalenko, K.; Krivokhizha, S.; Chaban, I. *JETP* **2009**, *108*, 866.

- (65) Comez, L.; Fioretto, D.; Scarponi, F.; Monaco, G. *J. Chem. Phys.* **2003**, *119*, 6032–6043.
- (66) Kearns, K. L.; Still, T.; Fytas, G.; Ediger, M. D. *Adv. Mater.* **2010**, *22*, 39.
- (67) Fabelinskii, I.; Sabirov, L.; Starunov, V. *Phys. Lett. A* **1969**, *29*, 414.
- (68) Dreyfus, C.; Aouadi, A.; Gapinski, J.; Matos-Lopes, M.; Steffen, W.; Patkowski, A.; Pick, R. M. *Phys. Rev. E* **2003**, *68*, 011204.
- (69) Monaco, G.; Fioretto, D.; Comez, L.; Ruocco, G. *Phys. Rev. E* **2001**, *63*, 061502.
- (70) Dreyfus, C.; Gupta, R.; Bonello, B.; Bousquet, C.; Taschin, A.; Ricci, M.; Pratesi, G. *J. Chem. Phys.* **2002**, *116*, 7323–7325.
- (71) Grimsditch, M.; Bhadra, R.; Torell, L. M. *Phys. Rev. Lett.* **1989**, *62*, 2616–2619.
- (72) Polian, A.; Vo-Thanh, D.; Richet, P. *Europhys. Lett.* **2002**, *57*, 375–381.
- (73) Youngman, R.; Kieffer, J.; Bass, J.; Duffrene, L. *J. Non-Cryst. Solids* **1997**, *222*, 190.
- (74) Hansen, J. P.; McDonald, I. R. *Theory of Simple Liquids*; Academic Press: New York, 1976.
- (75) Stickel, F.; Fischer, E. W.; Richert, R. *J. Chem. Phys.* **1996**, *104*, 2043–2055.
- (76) Sokolov, A. P.; Kisliuk, A.; Quitmann, D.; Kudlik, A.; Rössler, E. *J. Non-Cryst. Solids* **1994**, *172–174*, 138–153.
- (77) Richert, R.; Angell, C. A. *J. Chem. Phys.* **1998**, *108*, 9016–9026.
- (78) Hassan, A. K.; Torell, L. M.; Börjesson, L.; Doweidar, H. *Phys. Rev. B* **1992**, *45*, 12797–12805.
- (79) Soper, A. K. *J. Phys.: Condens. Mater.* **2010**, *22* (40), 404210.